Derjaguin-Landau-Verwey-Overbeek energy landscape of a Janus particle with a nonuniform cap

Siddharth Rajupet, Aidin Rashidi, and Christopher L. Wirth*
Department of Chemical and Biomolecular Engineering, Case School of Engineering, Case Western Reserve University, Cleveland, Ohio 44106, USA

(Received 18 December 2020; accepted 8 March 2021; published 29 March 2021)

A colloidal particle is often termed "Janus" when some portion of its surface is coated by a second material which has distinct properties from the native particle. The anisotropy of Janus particles enables unique behavior at interfaces. However, rigorous methodologies to predict Janus particle dynamics at interfaces are required to implement these particles in complex fluid applications. Previous work studying Janus particle dynamics does not consider van der Waals interactions and realistic, nonuniform coating morphology. Here we develop semianalytic equations to accurately calculate the potential landscape, including van der Waals interactions, of a Janus particle with nonuniform coating thickness above a solid boundary. The effects of both nonuniform coating thickness and van der Waals interactions significantly influence the potential landscape of the particle, particularly in high ionic strength solutions, where the particle samples positions very close to the solid boundary. The equations developed herein facilitate more simple, accurate, and less computationally expensive characterization of conservative interactions experienced by a confined Janus particle than previous methods.

DOI: 10.1103/PhysRevE.103.032610

I. INTRODUCTION

Micrometer scale colloidal particles often interact with solid boundaries [1–6], neighboring particles [7–9], or fluid interfaces [10–12]. The morphology and chemistry of particles significantly influence colloidal interactions, particularly when those properties are nonuniform over the particle surface. Such natural or synthetic anisotropic particles have gradually expanded in relevance [13]. A class of nonuniform colloidal particles, known as Janus particles, has shown increasing promise as building blocks for complex assemblies, active entities, or more generally in a wide array of complex fluid applications [14–16]. Janus particles are those particles that typically have some portion of their surface coated by a second material. The faces of a Janus particle often have significantly different characteristics that mediate unique dynamics while the particle is confined [17–20]. Controlling these phenomena experienced by Janus particles requires a methodology to predict interactions and dynamics at an interface.

Recent progress on simulations have revealed the dynamics of Janus spheres and rods [21,22], active Janus particles [23,24], Janus particles at fluid/fluid interfaces [25–27], and Janus particles responding to external flow or magnetic fields [28,29]. Moreover, studies simulating the Brownian dynamics of a Janus particle revealed how interfacial interactions experienced by Janus particles above a flat, solid substrate mediate dynamics [30,31]. These studies simulated the Brownian fluctuations in position and orientation of a polystyrene sphere with a uniformly thick gold coating on one hemisphere. Conservative interactions considered in these studies included the electric double layer (EDL) and gravitational forces on the Janus particle. Differences in the ζ potential between the two faces of the particle induced mild changes in the positions and orientations sampled, while gravitational torque caused by differences in density between the gold and polystyrene strongly quenched the particle orientation, particularly at larger particle sizes and coating thicknesses [31]. After Janus particle dynamics were characterized, procedures were developed to determine particle properties directly from data recording fluctuations in particle position and orientation [30].

Some aspects of this previous work can be expanded to better account for salient features of experimental systems. In particular, the studies summarized above did not include van der Waals (vdW) interactions, which are significant when a particle is in very close proximity to a solid boundary [32]. Furthermore, unlike those modeled in prior studies, synthesized Janus particles have coatings of nonuniform thickness by virtue of the fabrication process [33]. During fabrication, particle surface regions perpendicular to the direction of deposition typically acquire coatings with the expected thickness, while regions non-normal or parallel to the direction of deposition acquire thinner or no coating, respectively. Consequently, a more thorough model of real systems should include the effect of vdW interactions and nonuniform coating thickness.

Previous studies used a numerical meshing method to calculate the EDL force which cannot easily account for realistic cap morphology [30]. Herein, we summarize the development of a semianalytic model to calculate the Derjaguin-Landau-Verwey- Overbeek (DLVO) interactions of a Janus particle with a realistic coating morphology near a boundary. The expressions derived for the EDL, vdW, and gravitational potentials, are more accurate and less computationally intensive than methods used in previous Brownian dynamics studies. Furthermore, since the derived expressions are semianalytical, they are more readily applicable than previous numerical meshing methods.

*Corresponding author: wirth@case.edu

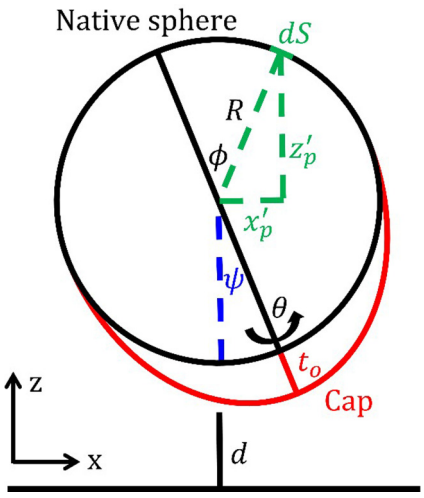

FIG. 1. Schematic of a Janus particle with cap of nonuniform thickness. The native particle is spherical, but the cap varies in thickness continuously from a maximum of t_o to zero. The separation distance between the native sphere and nearby boundary is equal to $d + t_o$.

II. THEORY

The Janus particle was modeled as a sphere of radius R with a coated region of thickness t which covers the region of the particle defined by the limits $\phi : \pi(1-c) \rightarrow \pi$ and $\theta : 0 \rightarrow 2\pi$ where ϕ and θ are the polar and azimuthal angle, respectively (see Fig. 1). Thus, c is the fractional surface coverage of the coated region and here we considered a Janus particle with $c = 0.5$. The underlying sphere of the Janus particle is termed the "native sphere", while the coated region is termed the "cap." Two cap morphologies were considered: a uniform cap with constant thickness such that $t = t_o$, and a cap with thickness varying as $t = t_o|\cos(\phi)|$ where t_o is the maximum thickness. This function was chosen as it approximates experimental measurements of typical cap thickness variation in Janus particles [33]. The orientation of the Janus particle is rotated by angle ψ such that $\psi = 0^\circ$ is the "cap-down" orientation and $\psi = 180^\circ$ is the "cap-up" orientation. The native sphere is separated from the flat substrate by a distance $d + t_o$ as depicted in Fig. 1.

We used the surface element integration (SEI) method to calculate the DLVO interaction energy of the Janus particle for different particle orientations [34]. The SEI method yields an exact solution for the DLVO interaction between an arbitrarily shaped object and a flat substrate. This method integrates the DLVO interaction between the parallel component of differential surface element dS and the flat substrate, which has an analytic solution, over the object's surface. The interaction energy U calculated from the SEI method is given by

$$U = \iint_S \mathbf{n} \cdot \mathbf{k} E(h) dS, \tag{1}$$

where $E(h)$ is the interaction energy per unit area between two parallel flat surfaces separated by distance h, $\mathbf{n}$ is the outward unit normal vector from the Janus particle element dS, and $\mathbf{k}$ is the unit vector in the z direction, perpendicular to the flat surface. Physically, $\mathbf{n} \cdot \mathbf{k} dS$ is the component of dS parallel to the flat substrate. This term can be expanded such that $\mathbf{n} \cdot \mathbf{k} = -z_p/r$, where z_p is the z position of dS relative to the center of the native sphere, and r is the radial distance between dS and center of the native sphere. The value of r depends on the position of dS; for dS on the native sphere, $r = R$, and for dS on the cap surface, $r = R + t$. The function for h is given as

$$h = z_p + R + t_o + d. \tag{2}$$

Particle orientation was accounted for by rotating the coordinate system about the y axis (into the page in Fig. 1), by angle ψ. The z position of dS after rotation, z_p', is adjusted such that $z_p' = z_p \cos(\psi) - x_p \sin(\psi)$, where x_p is the x position of dS relative to the center of the native sphere prior to rotation. The system was converted to spherical coordinates such that $dS = r^2 \sin(\phi) d\phi d\theta$, $z_p = r \cos(\phi)$ and $x_p = r \sin(\phi)\cos(\theta)$, where ϕ is the polar angle, and θ is the azimuthal angle. Adapting Eqs. (1) and (2) into spherical coordinates and accounting for rotation,

$$U = \iint_S -r^2 \sin(\phi)(\cos(\phi)\cos(\psi) - \sin(\phi)\cos(\theta)\sin(\psi))E(h) d\phi d\theta, \tag{3}$$

$$h = r\cos(\phi)\cos(\psi) - r\sin(\phi)\cos(\theta)\sin(\psi) + R + t_o + d. \tag{4}$$

The interaction energy per unit area between two flat plates due to the EDL interaction according to the linear superposition approximation is given by

$$E_{EDL} = B \exp(-\kappa h), \tag{5}$$

$$B = \frac{64 C_\infty kT \tanh\left(\frac{e\zeta_{\text{sub}}}{4kT}\right)\tanh\left(\frac{e\zeta_p}{4kT}\right)}{\kappa}, \tag{6}$$

where C_∞ is the bulk solution ionic strength, ζ_{sub} and ζ_p are the ζ potential of the substrate and particle, respectively, k is the Boltzmann constant, T is the temperature, e is the electronic charge, and κ is the inverse Debye length. The linear superposition approximation is most accurate when the double layers of the two surfaces are not overlapping; however, we emphasize that in our methodology, the approximation used for E_{EDL} can be adapted to best suit the system of interest. For example, other expressions relating the surface charge to the Stern potential (equated herein to the potential at the plane of shear, or the ζ potential) could be implemented.

Equation (5) was implemented into Eq. (3) by splitting the surface integral into two parts, namely one part that integrates over the uncapped, native sphere surface and a second part that integrates over the surface of the cap. For these two regions, the value of h and of constant B differs due to differences in r and ζ_p, respectively. For the native sphere region, $B = B_{\text{sph}}$ wherein $\zeta_p = \zeta_{\text{sph}}$, and $h = h_{\text{sph}}$ wherein $r = R$. For the capped region $B = B_{\text{cap}}$ wherein $\zeta_p = \zeta_{\text{cap}}$, and $h = h_{\text{cap}}$ wherein $r = R + t$. As such, the EDL interaction potential, U_{EDL}, is given as

$$U_{EDL}^{\text{sph}} = \int_0^{2\pi} \int_0^{\pi(1-c)} -R^2 \sin(\phi)(\cos(\phi)\cos(\psi) - \sin(\phi)\cos(\theta)\sin(\psi))B_{\text{sph}} \exp(-\kappa h_{\text{sph}}) d\phi d\theta, \tag{7a}$$

$$U_{EDL}^{\text{cap}} = \int_0^{2\pi}\int_{\pi(1-c)}^{\pi} -(R+t)^2\sin(\phi)(\cos(\phi)\cos(\psi) - \sin(\phi)\cos(\theta)\sin(\psi))B_{\text{cap}}\exp(-\kappa h_{\text{cap}})d\phi d\theta, \tag{7b}$$

$$U_{EDL} = U_{EDL}^{\text{sph}} + U_{EDL}^{\text{cap}}. \tag{7c}$$

We use the SEI method to also determine the vdW interaction with the cap of the Janus particle. The vdW interaction energy per unit area between two flat plates is given by

$$E_{VDW} = -\frac{A}{12\pi h^2}, \tag{8}$$

where A is the Hamaker constant. To find the vdW interaction energy due to the cap, we insert Eq. (8) in Eq. (3) with $A = A_{\text{cap}}$. To account for the fact that the cap is a thin shell, we integrate Eq. (3) over the exterior of the cap, and then subtract Eq. (3) integrated over the interior of the cap. Note that the same Hamaker constant must be used for the exterior and interior of the cap. Thus the vdW interaction energy due to the cap is given as

$$U_{VDW}^{\text{cap}} = \frac{A_{\text{cap}}}{12\pi}\int_0^{2\pi}\int_{\pi(1-c)}^{\pi}\sin(\phi)(\cos(\phi)\cos(\psi) - \sin(\phi)\cos(\theta)\sin(\psi))\left[\frac{(R+t)^2}{h_{\text{cap}}^2} - \frac{R}{h_{\text{sph}}^2}\right]d\phi d\theta. \tag{9a}$$

The vdW interaction energy between the native sphere and a flat substrate has an analytic solution,

$$U_{VDW}^{\text{sph}} = -\frac{A_{\text{sph}}}{6}\left[\frac{R}{d+t_o} + \frac{R}{d+t_o+2R} + \ln\left(\frac{d+t_o}{d+t_o+2R}\right)\right], \tag{9b}$$

and the total vdW interaction energy of the Janus particle is

$$U_{VDW} = U_{VDW}^{\text{sph}} + U_{VDW}^{\text{cap}}. \tag{9c}$$

Finally, the gravitational potential of the native sphere is given by

$$U_G^{\text{sph}} = \frac{4}{3}g(\rho_{\text{sph}} - \rho_f)\pi R^3(d + t_o + R), \tag{10a}$$

where ρ_{sph} and ρ_f are the densities of the native sphere and fluid, respectively, and g is the gravitational constant. The gravitational potential of the cap, which has density ρ_{cap}, is given by

$$U_G^{\text{cap}} = g(\rho_{\text{cap}} - \rho_f)\int_0^{2\pi}\int_{\pi(1-c)}^{\pi}\int_R^{R+t} hr^2\sin(\phi)drd\phi d\theta \tag{10b}$$

and

$$U_G = U_G^{\text{sph}} + U_G^{\text{cap}}. \tag{10c}$$

In the case of a uniform cap such that $t = t_o$, the triple integral in Eq. (10b) has an analytic solution,

$$U_G^{\text{cap}} = g(\rho_{\text{cap}} - \rho_f)\left[\frac{1}{12}\pi t_o(-8(d + t_o + R) \times \left(3R^2 + 3Rt_o + t_o^2\right)(-1 - \cos(\pi - c\pi)) - 3(2R + t_o)\left(2R^2 + 2Rt_o + t_o^2\right)\cos(\psi)\sin^2(c\pi))\right]. \tag{10d}$$

In our calculations, we used physical properties characteristic of silica for the substrate, polystyrene for the native sphere, gold for the cap, and an aqueous monovalent salt solution for the medium. As such, the density, ρ, Hamaker constant, A, and the ζ potential, ζ, of the native sphere are $\rho_{\text{sph}} = 1055\,\text{kg/m}^3$, $A_{\text{sph}} = 9.28\times10^{-21}\,\text{J}$, and $\zeta_{\text{sph}} = -50\,\text{mV}$ respectively, that of the cap are $\rho_{\text{cap}} = 19320\,\text{kg/m}^3$, $A_{\text{cap}} = 2.55\times10^{-20}\,\text{J}$ and $\zeta_{\text{cap}} = -5\,\text{mV}$ respectively, and the ζ potential of the substrate is $\zeta_{\text{sub}} = -50\,\text{mV}$.

The method described herein used an approximation to calculate the potential of the cap in each the uniform and nonuniform cap cases, which introduces some error with respect to the exact solution. First, in the uniform cap case, the integral is not conducted over the surface edge of the cap, at the boundary between the capped region and uncapped region of the Janus particle. Neglecting this portion of the cap will only affect the vdW interaction which is a volume interaction. The integral must be conducted over the full, closed surface of the cap to properly account for the volume. Next, in the nonuniform cap case, the normal vector to the cap, **n**, is assumed to be in the same direction as the radial vector from the native sphere center to dS, **r**. This assumption affects both vdW and EDL calculations, but will only introduce error in the case of the nonuniform cap in which the cap deviates from spherical curvature more significantly toward the edges of the cap.

We characterize the error due to these approximations and validate our model by comparison to the exact numerical solution of the vdW potential for the Janus particle. To calculate the exact solution of U_{VDW}^{cap}, we integrate the interaction between a point and flat substrate, which has an analytic solution [35] over the volume of the cap. The error due to both approximations in our model becomes more significant as d and t_o become large relative to R. The error associated with these approximations is ∼1% error for a Janus particle with $R = 1\,\mu\text{m}$ and $t_o = 20\,\text{nm}$, when $d = 100\,\text{nm}$, characteristic of a typical experimental system.

III. RESULTS

A. Influence of van der Waals interactions

Given that no previous work has incorporated vdW interactions between a Janus particle and nearby boundary, we first characterized the influence of vdW interactions on the potential energy profile experienced by a uniform-capped Janus particle. We calculated the potential energy profile of the particle in the cap-down orientation with and without the inclusion of vdW interactions [see Fig. 2(a)]. Here, vdW interactions shift the secondary minimum of the potential landscape,

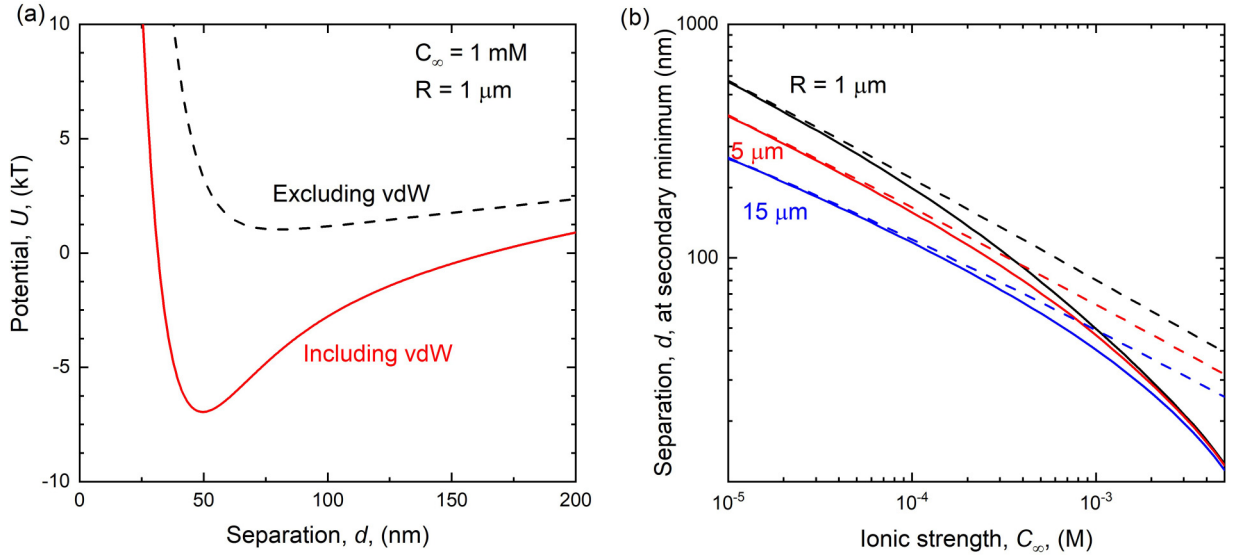

FIG. 2. (a) Potential distribution of a uniform-capped particle in the cap-down orientation ($\psi = 0$) with $R = 1$ μm and $t_o = 20$ nm in a 1-mM ionic strength solution including vdW interactions (red solid) and excluding vdW interactions (black dashed), (b) particle-substrate separation, d, at the secondary minima of the potential landscape including vdW interactions (solid) and excluding vdW interactions (dashed) for a uniform-capped particle in the cap-down orientation ($\psi = 0$) with $t_o = 20$ nm and $R = 1$ μm (black), 5 μm (red), and 15 μm (blue).

characteristic of the most probable particle position, closer to the substrate and narrows and deepens the potential well. Physically, the narrower potential well causes positions sampled by the particle to be more localized to the secondary minimum. For instance, excluding vdW interactions, the particle could feasibly sample positions greater than 200 nm from the substrate due to Brownian fluctuations, whereas when vdW interactions are included, the particle can only feasibly sample positions between ~40 and 75 nm from the substrate.

Next, we characterized conditions wherein vdW interactions are significant by calculating the particle separation at the secondary minimum of the potential landscape with and without the inclusion of vdW interactions [see Fig. 2(b)]. At the secondary minima, repulsive forces, consisting of EDL interactions, balance attractive forces, consisting of gravitational and vdW interactions. Thus, vdW interactions will only be significant at the secondary minima when they are comparable to, or greater than gravitational forces.

At very low ionic strength, and correspondingly large Debye length, the particle will sample positions far from the nearby boundary causing inclusion of vdW interactions to have little effect on the position of the secondary minimum. At higher ionic strengths the particle will sample positions closer to the substrate where vdW forces rival gravitational forces; thus, in this regime, vdW interactions significantly shift the secondary minimum closer to the substrate. Under these conditions, vdW interactions also significantly deepen and narrow the potential well as discussed above. Continuing to increase the ionic strength beyond ~5 mM will induce deposition because the EDL energy barrier has been sufficiently diminished. Since gravitational forces on the particle scale with R^3 while vdW forces scale with $\sim R$, the influence of vdW interactions is more significant at smaller particle sizes where vdW forces are larger relative to gravitational forces.

B. Influence of cap nonuniformity

Next, the model was extended to Janus particles with a nonuniform cap. We found nonuniformity of cap thickness to profoundly impact variation of interaction energy with particle orientation (see Fig. 3). The cap nonuniformity has three main effects on the variation of interaction energy with orientation. First, a nonuniform cap changes the particle-substrate separation for a given $d + t_o$ while orientation is varied. Second, a nonuniform cap has a smaller volume (and thus smaller total mass) as compared to a uniform cap of the same nominal thickness. Finally, a nonuniform cap concentrates more volume (and thus more mass) to the center of the cap at the expense of the edges.

The EDL interaction is only influenced by the first effect, that of the separation distance, since the interaction is a surface, as opposed to a volume, phenomenon. As shown in Fig. 3(a), both the uniform and nonuniform cap have a higher potential in the cap-down orientation than the cap-up orientation, despite the cap having a ζ potential magnitude less than that of the native sphere. The reason for this effect is that the particle-substrate separation distance for a given $d + t_o$ is smaller in the cap-down orientation than the cap-up orientation, making the EDL interaction stronger in the cap-down position. However, in contrast to the uniform cap case, there is a minimum EDL energy in the nonuniform cap case around an orientation of ~80°. At this orientation, the cap is facing the substrate in both uniform and nonuniform cases, but in the nonuniform case, the region of the cap facing the substrate is very thin, so the separation between the particle and substrate is larger, thereby reducing the interaction potential. In this regime of orientations, the nonuniform cap potential closely resembles that of a particle with an infinitely thin cap positioned such that the native sphere is equally separated from the substrate [dotted-line in Fig. 3(a)]. In this case of an infinitely thin cap, the two sides

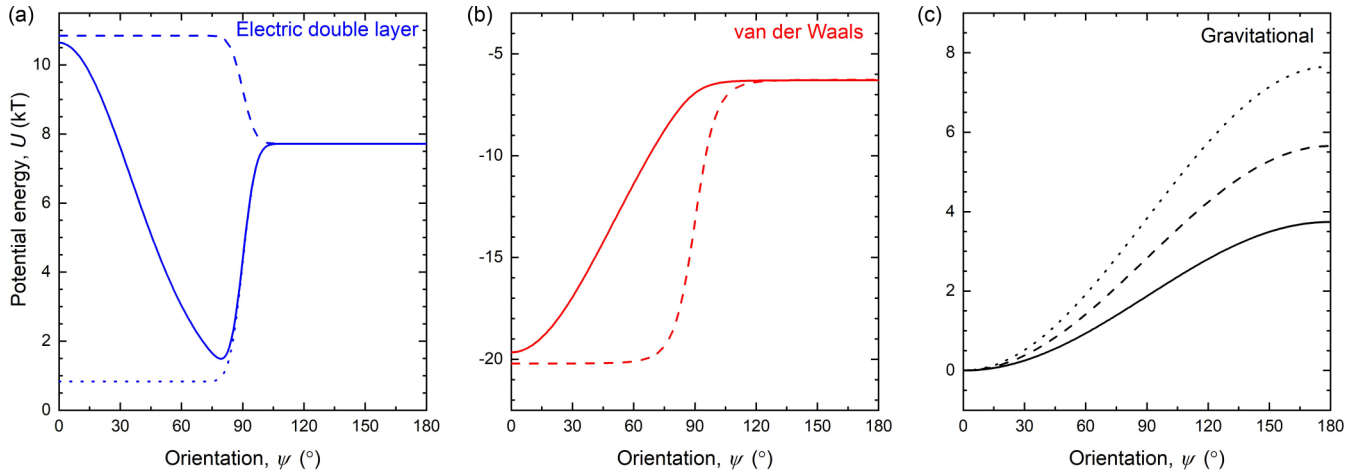

FIG. 3. Potential energy of a Janus particle with $R = 1\,\mu$m and $t_o = 20$ nm near a boundary as a function of polar orientation in a 5-mM ionic strength solution at fixed $d = 30$ nm for (a) electric double layer, (b) van der Waals, and (c) gravitational interactions. The dashed curve is for a uniform cap and the solid curve a nonuniform cap. The dotted curve in (a) is for a particle with $t_o \to 0$ and $d = 50$ nm. The dotted curve in (c) is for a Janus particle with a nonuniform cap and $t_o = 40$ nm such that its mass matches that of the uniform cap case with $t_o = 20$ nm. Gravitational potentials in (c) have been shifted such that $U = 0$ at $\psi = 0$. Note for each interaction there is a profound impact of cap uniformity on the conservative interaction.

of the particle have different surface composition causing the potential to vary with orientation, but the particle-substrate separation does not vary with orientation due to the thinness of the cap.

The impact of cap nonuniformity on separation distance is most influential for the vdW interaction because of its rapid decay with distance. Similar to the EDL interaction, for the vdW interaction, the potential of the nonuniform cap approaches that of the uniform cap in the limits of the cap-down and cap-up orientations. This effect occurs since in both the EDL and vdW interaction, the potential depends strongly on the separation distance. In the cap-down orientation, the DLVO interaction is dominated by the center region of the cap, which has the same separation from the substrate in the uniform and nonuniform cases. However, in the cap-up orientation, the DLVO interaction is dominated by the native sphere contribution, which is not affected by the cap morphology. As the particle rotates from $\psi = 0^\circ$ at a fixed $d + t_o$, the separation between the particle and substrate increases in the nonuniform case, but remains the same until the edge of the cap in the uniform case. As a result, the vdW potential increases continuously as the particle rotates from the cap-down orientation in the nonuniform case, but only increases once the edge of the cap is facing the substrate, at $\psi = 90^\circ$, in the uniform case. Physically, this causes the particle to be more quenched in the cap-down orientation due to vdW interactions in the nonuniform case.

The latter two effects, those of the total and distribution of cap mass, are most influential for the gravitational potential, yet influence the potential energy in opposing ways. Since a nonuniform cap with equal t_o to a uniform cap has less mass, the gravitational potential due to the nonuniform cap will vary less with orientation, as seen in Fig. 3(c). However, since the nonuniformity distributes more mass to the center of the cap, which is the furthest from the substrate in the cap-up orientation, the gravitational potential increases more rapidly with orientation for a nonuniform cap than uniform cap when both caps have the same total mass [Fig. 3(c), dotted line vs dashed line].

For caps of equal nominal thickness, nonuniformity has opposing effects on the vdW and the gravitational potentials. Cap nonuniformity more strongly quenches particle orientations in the cap-down position due to vdW interactions and less strongly quenches orientations due to gravitational interactions. As such, in regimes when gravitational interactions are dominant over vdW interactions, nonuniformity decreases quenching, allowing the particle to sample more orientations, and when vdW interactions are dominant, nonuniformity increases quenching. Since vdW interactions decay with increasing separation distance and gravitational interactions are independent of separation distance, vdW interactions dominate at small separations, while gravitational interactions dominate at large separations.

This effect can be observed in Fig. 4, which depicts the potential landscape of a Janus particle above a boundary with a uniform cap [Fig. 4(a)] and the landscape with a nonuniform cap [Fig. 4(b)]. For instance, at the secondary minimum, where the separation distance is small and vdW interactions are dominant, the particle can sample a wider range of orientations in the uniform case as compared to the nonuniform case. This effect is even more pronounced at the primary minimum, where the range of possible orientations at deposition is far more limited in the nonuniform case than the uniform case. On the other hand, at large separation distances, where gravitational interactions are dominant, the particle can sample a wider range of orientations in the nonuniform case than in the uniform case. In addition, since the cap has less mass in the nonuniform case, the particle can sample a larger array of particle positions from the substrate.

We emphasize the effects of vdW interactions and cap nonuniformity are most pronounced at small separation distances. At large separation distances, vdW interactions will be small relative to gravitational interactions, and possibly EDL interactions depending on the ionic strength of the solution.

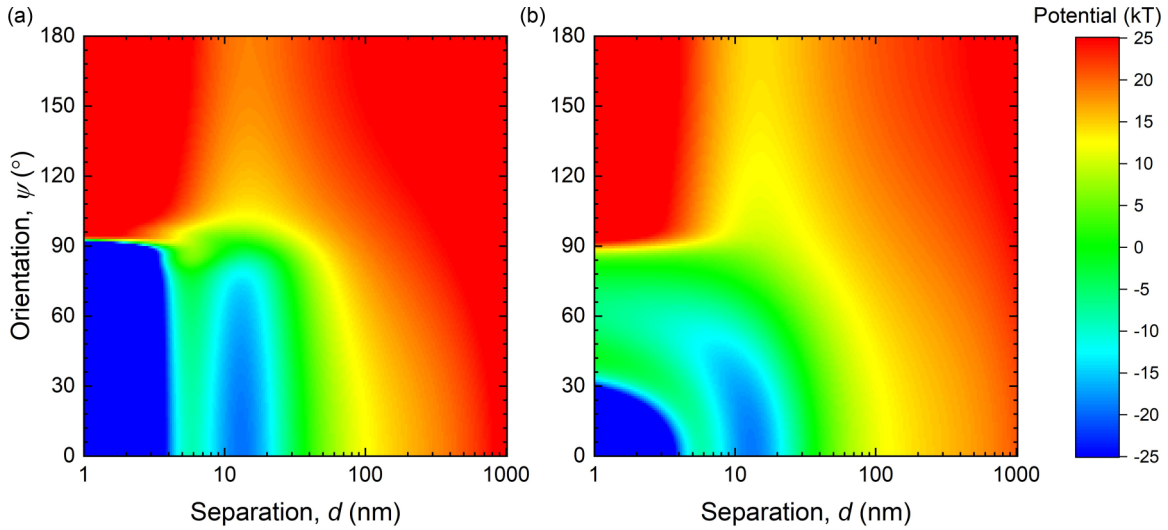

FIG. 4. Total potential energy landscape for a Janus particle with $R = 1\ \mu$m and $t_o = 20$ nm near a substrate in a 5-mM solution in which the particle has a (a) uniform or (b) nonuniform cap.

When d is large relative to t_o the effect of cap nonuniformity will be less pronounced since changes in separation distance with orientation will be less significant.

C. Extended applications of the model

We have shown cap nonuniformity and vdW interactions impact the potential landscape of a Janus particle most significantly at small separation distances. However, substrate roughness, even on the nanoscale, has been shown to greatly affect the DLVO interactions on particles, particularly at small separation distances [36–38], and is often credited for discrepancies between theoretical and experimental energy profiles [39–41]. While characterizing effects of substrate roughness on Janus particle dynamics is beyond the scope of the present article, the model developed herein can be extended to account for the substrate morphology. Following the work of Hoek *et al.* [36], the present model can be adapted to calculate DLVO interactions between the Janus particle and a rough substrate, described by function $f(x,y)$, by modifying h in Eq. (4) such that h is the vertical distance between dS on the particle and the rough substrate below it,

$$h = r\cos(\phi)\cos(\psi) - r\sin(\phi)\cos(\theta)\sin(\psi) + R + t_o + d - f(x_p', y_p), \tag{11}$$

where x_p' is the x position of dS after rotation about the y axis, given by $x_p' = x_p\cos(\psi) + z_p\sin(\psi)$, and y_p is the y position of dS, which does not change with orientation. Note that to implement Eq. (11) into Eq. (3), x_p, y_p, and z_p must be converted into spherical coordinates.

Our model can also be extended for use in Brownian dynamics simulations which input the conservative forces acting on the particle. Thus far we have derived the DLVO energy of a particle near substrate, but our model can be adapted to calculate the forces acting on the particle by substituting $E(h)$ in Eq. (3) for the vdW or EDL pressure between two flat plates, $\Pi(h)$. Due to the low computational requirements of the model, it is well suited for application in Brownian dynamics simulations which require calculation of conservative interactions for up to millions of time steps [30,31].

IV. CONCLUSION

In conclusion, we developed a semianalytic expression to calculate the DLVO and gravitational potentials of a Janus particle with nonuniform cap thickness above a boundary for different particle orientations. We find that at small separation distances, which are particularly relevant in high ionic strength solutions, van der Waals interactions, and cap nonuniformity significantly influence the particle's potential landscape. The methods developed herein are significant since they provide equations of utility suitable for modeling conservative interactions experienced by a confined Janus particle.

ACKNOWLEDGMENTS

This work was supported by the National Science Foundation CAREER Award, NSF No. 2023525. S.R. developed and implemented the methodology. S.R., A.R., and C.L.R. determined the data to collect for the figures and analyzed and discussed this data. S.R., A.R., and C.L.R. contributed to writing and editing the manuscript.

[1] D. C. Prieve, P. J. Sides, and C. L. Wirth, 2D assembly of colloidal particles on a planar electrode, Curr. Opin. Colloid Interface Sci. **15**, 160 (2010).

[2] H. J. Wu, W. N. Everett, S. G. Anekal, and M. a. Bevan, Mapping patterned potential energy landscapes with diffusing colloidal probes, Langmuir **22**, 6826 (2006).

[3] M. A. Bevan and D. C. Prieve, Forces and hydrodynamic interactions between polystyrene surfaces with adsorbed PEO−PPO−PEO, Langmuir **16**, 9274 (2000).

[4] H. Brenner, The slow motion of a sphere through a viscous a plane surface, Chem. Eng. Sci. **16**, 242 (1961).

[5] S. Biggs, D. C. Prieve, and R. R. Dagastine, Direct comparison of atomic force microscopic and total internal reflection microscopic measurements in the presence of nonadsorbing polyelectrolytes, Langmuir **21**, 5421 (2005).

[6] S. Das, A. Garg, A. I. Campbell, J. Howse, A. Sen, D. Velegol, R. Golestanian, and S. J. Ebbens, Boundaries can steer active janus spheres, Nat. Commun. **6**, 8999 (2015).

[7] H. J. Wu, T. O. Pangburn, R. E. Beckham, and M. a. Bevan, Measurement and interpretation of particle-particle and particle-wall interactions in levitated colloidal ensembles, Langmuir **21**, 9879 (2005).

[8] S. Sacanna, W. T. M. Irvine, P. M. Chaikin, and D. J. Pine, Lock and key colloids, Nature (London) **464**, 575 (2010).

[9] B. Tränkle, M. Speidel, and A. Rohrbach, Interaction dynamics of two colloids in a single optical potential, Phys. Rev. E **86**, 021401 (2012).

[10] T. G. Anjali and M. G. Basavaraj, Contact angle and detachment energy of shape anisotropic particles at fluid-fluid interfaces, J. Colloid Interface Sci. **478**, 63 (2016).

[11] W. Fei, Y. Gu, and K. J. M. Bishop, Active colloidal particles at fluid-fluid interfaces, Curr. Opin. Colloid Interface Sci. **32**, 57 (2017).

[12] M. Oettel and S. Dietrich, Colloidal interactions at fluid interface, Langmuir **24**, 1425 (2008).

[13] S. C. Glotzer and M. J. Solomon, Anisotropy of building blocks and their assembly into complex structures, Nat. Mater. **6**, 557 (2007).

[14] A. B. Pawar and I. Kretzschmar, Fabrication, assembly, and application of patchy particles, Macromol. Rapid Commun. **31**, 150 (2010).

[15] J. Zhang, B. A. Grzybowski, and S. Granick, Janus particle synthesis, assembly, and application, Langmuir **33**, 6964 (2017).

[16] S. Razavi, K. D. Cao, B. Lin, K. Y. C. Lee, R. S. Tu, and I. Kretzschmar, Collapse of particle-laden interfaces under compression: buckling vs particle expulsion, Langmuir **31**, 7764 (2015).

[17] S. E. Spagnolie and E. Lauga, Hydrodynamics of self-propulsion near a boundary: Predictions and accuracy of far-field approximations, J. Fluid Mech. **700**, 105 (2012).

[18] I. Kretzschmar and J. H. (Kevin) Song, Surface-anisotropic spherical colloids in geometric and field confinement, Curr. Opin. Colloid Interface Sci. **16**, 84 (2011).

[19] I. Buttinoni, J. Bialké, F. Kümmel, H. Löwen, C. Bechinger, and T. Speck, Dynamical Clustering and Phase Separation in Suspensions of Self-Propelled Colloidal Particles, Phys. Rev. Lett. **110**, 238301 (2013).

[20] M. A. Fernandez-Rodriguez, M. A. Rodriguez-Valverde, M. A. Cabrerizo-Vilchez, and R. Hidalgo-Alvarez, Surface activity of Janus particles adsorbed at fluid–fluid interfaces: Theoretical and experimental aspects, Adv. Colloid Interface Sci. **233**, 240 (2016).

[21] A. Kharazmi and N. V. Priezjev, Molecular dynamics simulations of the rotational and translational diffusion of a janus rod-shaped nanoparticle, J. Phys. Chem. B **121**, 7133 (2017).

[22] A. Kharazmi and N. V. Priezjev, Diffusion of a janus nanoparticle in an explicit solvent: A molecular dynamics simulation study, J. Chem. Phys. **142**, 234503 (2015).

[23] D. Chakraborty, Orientational dynamics of a heated janus particle, J. Chem. Phys. **149**, 174907 (2018).

[24] L. Theeyancheri, S. Chaki, N. Samanta, R. Goswami, R. Chelakkot, and R. Chakrabarti, Translational and rotational dynamics of a self-propelled janus probe in crowded environments, Soft Matter **16**, 8482 (2020).

[25] J. Koplik and C. Maldarelli, Molecular dynamics study of the translation and rotation of amphiphilic janus nanoparticles at a vapor-liquid surface, Phys. Rev. Fluids **4**, 044201 (2019).

[26] S. Razavi, J. Koplik, and I. Kretzschmar, Molecular dynamics simulations: Insight into molecular phenomena at interfaces, Langmuir, **30**, 11272 (2014).

[27] D. Wang, Y.-L. Zhu, Y. Zhao, C. Y. Li, A. Mukhopadhyay, Z.-Y. Sun, K. Koynov, and H.-J. Butt, Brownian diffusion of individual janus nanoparticles at water/oil interfaces, ACS Nano **14**, 10095 (2020).

[28] S. Safaei, A. Y. M. Archereau, S. C. Hendy, and G. R. Willmott, Molecular dynamics simulations of janus nanoparticles in a fluid flow, Soft Matter **15**, 6742 (2019).

[29] T. W. Long, U. M. Córdova-Figueroa, and I. Kretzschmar, Measuring, modeling, and predicting the magnetic assembly rate of 2D-staggered janus particle chains, Langmuir **35**, 8121 (2019).

[30] A. Rashidi and C. L. Wirth, Motion of a janus particle very near a wall, J. Chem. Phys. **147**, 224906 (2017).

[31] A. Rashidi, S. Razavi, and C. L. Wirth, Influence of cap weight on the motion of a janus particle very near a wall, Phys. Rev. E **101**,042606 (2020).

[32] D. C. Prieve, Measurement of colloidal forces with TIRM, Adv. Colloid Interface Sci. **82**, 93 (1999).

[33] A. Rashidi, M. W. Issa, I. T. Martin, A. Avishai, S. Razavi, and C. L. Wirth, Local measurement of janus particle cap thickness, ACS Appl. Mater. Interfaces **10**, 30925 (2018).

[34] S. Bhattacharjee and M. Elimelech, Surface element integration: A novel technique for evaluation of DLVO interaction between a particle and a flat plate, J. Colloid Interface Sci. **193**, 273 (1997).

[35] J. N. Israelachvili, *Intermolecular and Surface Forces* (Academic Press, New York, 2011).

[36] E. M. V. Hoek, S. Bhattacharjee, and M. Elimelech, Effect of membrane surface roughness on colloid−membrane DLVO interactions, Langmuir **19**, 4836 (2003).

[37] C. Shen, F. Wang, B. Li, Y. Jin, L.-P. Wang, and Y. Huang, Application of DLVO energy map to evaluate interactions between spherical colloids and rough surfaces, Langmuir **28**, 14681 (2012).

[38] S. Rajupet, M. Sow, and D. J. Lacks, Particle adhesion to rough surfaces, Phys. Rev. E **102**, 012904 (2020).

[39] X. Huang, S. Bhattacharjee, and E. M. V. Hoek, Is surface roughness a "scapegoat" or a primary factor when defining particle−substrate interactions? Langmuir **26**, 2528 (2010).

[40] L. Suresh and J. Y. Walz, Effect of surface roughness on the interaction energy between a colloidal sphere and a flat plate, J. Colloid Interface Sci. **183**, 199 (1996).

[41] M. A. Bevan and D. C. Prieve, Direct measurement of retarded van der Waals attraction, Langmuir **15**, 7925 (1999).